194
11-3-75

OR-1714

UCRL-51869

# EXPOSURE OF HIGH-TEMPERATURE ALLOYS IN CARBONACEOUS GAS ATMOSPHERES

A. Goldberg

A. J. Perkins

September 9, 1975

Prepared for U.S. Energy Research & Development Administration under contract No. W-7405-Eng-48

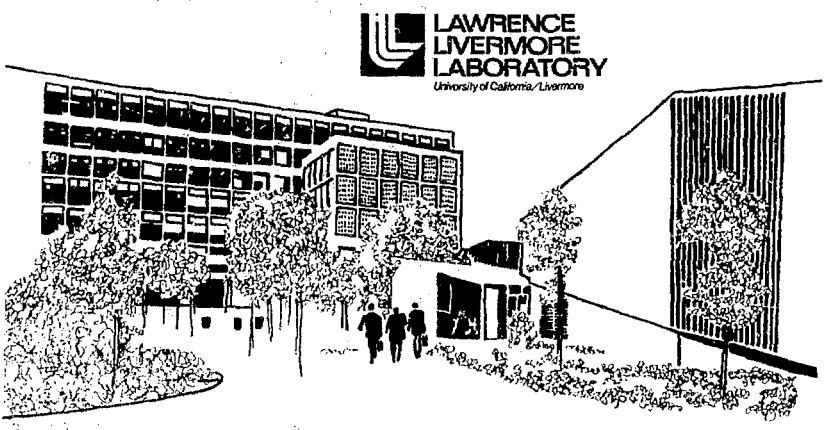


MASTER

DISTRIBUTION OF THIS DOCUMENT IS UNLIMITED

NOTICE

"This report was prepared as an account of work sponsored by the United States Government. Neither the United States nor the United States Energy Research & Development Administration, nor any of their employees, nor any of their contractors, subcontractors, or their employees, makes any warranty, express or implied, or assumes any legal liability or responsibility for the accuracy, completeness or usefulness of any information, apparatus, product or process disclosed, or represents that its use would not infringe privately-owned rights."

Printed in the United States of America
Available from
National Technical Information Service
U.S. Department of Commerce
5285 Port Royal Road
Springfield, Virginia 22151
Price: Printed Copy $___*; Microfiche $2.25

| *Pages | NTIS Selling Price |
|---|---|
| 1-50 | $4.00 |
| 51-150 | $5.45 |
| 151-325 | $7.60 |
| 326-500 | $10.60 |
| 501-1000 | $13.60 |

Distribution Category
UC-25

LAWRENCE LIVERMORE LABORATORY
University of California/Livermore, California/94550

UCRL-51869

# EXPOSURE OF HIGH-TEMPERATURE ALLOYS IN CARBONACEOUS GAS ATMOSPHERES

A. Goldberg

A. J. Perkins

MS. Date: September 9, 1975

NOTICE

This report was prepared as an account of work sponsored by the United States Government. Neither the United States nor the United States Energy Research and Development Administration, nor any of their employees, nor any of their contractors, subcontractors, or their employees, makes any warranty, express or implied, or assumes any legal liability or responsibility for the accuracy, completeness or usefulness of any information, apparatus, product or process disclosed, or represents that its use would not infringe privately owned rights.

DISTRIBUTION

# Contents

# EXPOSURE OF HIGH TEMPERATURE ALLOYS IN CARBONACEOUS GAS ATMOSPHERES


## Abstract

We used light and scanning electron microscopy to evaluate changes resulting from exposure of eight commercial high temperature alloys in carbonaceous atmospheres. Samples were exposed in CO, $CH_4$, or $CO/CH_4$ mixtures up to 900°C and 6.2 MPa. All alloys were actively attacked. Surface finish and preoxidation influenced the extent of corrosion. Reduction of NiO, giving a high surface concentration of Ni, promoted catalytic decomposition of $CH_4$. Further work is indicated before the performance of these alloys may be ranked with confidence.



## Summary

Although much information exists on the behavior of high-temperature, corrosion-resistant alloys in oxygen-rich environments, information on the behavior of these materials in carbonaceous atmospheres is scarce. The corrosion resistance of these alloys is due to the protection offered by their oxide surface films. The stability of such films in carbonaceous atmospheres will depend on the gas composition (e.g., $CO/CO_2$ ratio), temperature, and pressure with the oxides of Ni, Fe, Cr, and Al tending to be more stable, in that order.

In the present study we evaluated the metallurgical changes resulting from exposure of eight commercial alloys (Table 1) in high-temperature, high-pressure, carbonaceous gas atmospheres (Table 2). Either pure CO, pure $CH_4$, or a $CO/CH_4$ mixture was charged into a pressure vessel containing the exposed samples. On raising the temperature these charges decomposed to $CO/CO_2$, $CH_4/H_2$ and $CO/CO_2/CH_4/H_2$ mixtures, respectively.

For the combination of pressure, temperature, and $CO/CO_2$ ratios obtained, NiO would be unstable and it should be reduced if at the surface. Some form of iron oxide will be stable with the exact oxide species depending upon the particular environmental conditions. Both $Cr_2O_3$ and $Cr_{23}C_6$ should be stable in all cases. $Al_2O_3$ will be the most stable of these oxides and the Al will not form a carbide. Neither Ni nor Fe should form carbides in the environments examined.

We investigated both the effect of surface roughness and a preoxidation treatment. The exposed samples were evaluated

Table 1 -- Nominal Alloy Compositions (wt%)

| Alloy | Fe | Cr | Ni | C | Al | Mo | Other |
|---|---|---|---|---|---|---|---|
| 304 SS | Bal | ≥18 | ≥ 8 | ≤0.08 | -- | -- | -- |
| 310 SS | Bal | 26 | 20 | ≤0.25 | -- | -- | -- |
| Inconel 601 | Bal | 23 | 60 | 0.05 | 1.35 | -- | -- |
| Incoloy 800 | Bal | 20 | 34 | 0.07 | 0.5 | -- | -- |
| Incoloy 811 | Bal | 20 | 34 | 0.06 | 1.85 | | Ti(0.5) |
| Haynes 188 | 1.5 | 22 | 22 | 0.08 | -- | -- | Co(Bal),W(14) |
| E-brite 26-1 | Bal | 26 | -- | ≤0.01 | -- | 1 | -- |
| Hastelloy X | 19 | 22 | Bal | 0.1 | -- | 9 | Co(2) |

Table 2. High-temperature, high-pressure carbonaceous mixed gas atmospheres.

| Run No | Gas analysis | | | | | | Temp. (°C) | Press. (MPa) | Time (h) |
|---|---|---|---|---|---|---|---|---|---|
| | Initial | | Final | | | | | | |
| | CO | $CH_4$ | CO | $CO_2$ | $CH_4$ | $H_2$ | | | |
| 1 | -- | 100 | 0.2 | 0.15 | 98.1 | 1.07 | 600 | 4.8 | 170 |
| 2 | -- | 100 | -- | -- | 46.1 | 53.8 | 800 | 4.1 | 100 |
| 3 | -- | 100 | -- | -- | 42.2 | 57.6 | 900 | 4.8 | 50 |
| 4 | 100 | -- | 17.7 | 74.7 | 4.39 | 1.39 | 600 | 4.5 | 170 |
| 5 | 100 | -- | 34.8 | 63.4 | 0.06 | 0.91 | 800 | 4.5 | 170 |
| 6 | -- | 100 | 0.06 | 0.04 | 75.8 | 24.1 | 700 | 4.8 | 100 |
| 7 | 50 | 50 | 14.1 | 20.7 | 52.3 | 12.8 | 700 | 4.1 | 100 |
| 8 | 50 | 50 | 15.2 | 21.6 | 52.5 | 10.6 | 700 | 5.5 | 100 |
| 9 | 50 | 50 | 13.2 | 18.7 | 52.3 | 15.8 | 700 | 6.2 | 100 |
| 10 | 100 | -- | 18.14 | 80.5 | 0 | 0.41 | 700 | 6.2 | 100 |

using primarily light microscopy and scanning electron microscopy. Light microscopy generally revealed that three corrosion/diffusion zones had developed in all of the atmospheres examined. These were usually seen as 1) a structureless grey etching layer, 2) a sublayer consisting of small equiaxed light-etching grains; and 3) below this a region of general precipitation and/or grain boundary precipitation in the base metal.

Whether preoxidation reduced the extent of penetration of corrosive products into the base metal depended upon the preoxidation temperature (in air) and the alloy. An increase in surface roughness (as-machined vs 600-grit polish) greatly increased the extent of penetration and density of corrosion products. Details of the surface films are described with reference to scanning electron microscopy.

NiO, first formed by preoxidation, is selectively reduced when exposed to the carbonaceous atmosphere and soot invariably forms. A possible cause of soot formation may be catalytic action of nickel in cracking the gas. Detailed examination of the surface films indicates that carbonaceous gases may have a devastating effect on the performance of contemporary alloys.

Although the limited scope of the present investigation prevents ranking the various alloys examined, it did provide information on the type of corrosion caused by simple carbonaceous-gas atmospheres. The observations will serve as a basis for future studies on corrosion in the more complex coal gasification environments. However, to adequately understand the corrosion behavior and to accurately rank tested materials, the corrosion products must be identified and the extent of solute depletion as a function of substrate depth must be obtained. Finally, changes in mechanical properties due to synergistic effects of stress and corrosion will have to be assessed.

## Introduction

Much of our knowledge concerning the resistance of stainless steels and heat-resistant alloys to high-temperature gaseous corrosion is derived from studies of simple oxidation behavior, generally related to furnace and gas-turbine applications. A number of excellent reviews on various aspects of corrosion behavior for these materials have been published.[1-6] However, little research has been done on their behavior in carbonaceous reducing atmospheres such as those encountered in coal burning and coal gasification.[7-9] These atmospheres may contain, for example, CO, $CH_4$, $CO_2$, H, and $H_2O$ in various proportions at high temperature.

Classical approaches to corrosion resistance in oxidizing atmospheres may not apply for carbonaceous atmospheres. The approach to high temperature corrosion resistance has centered on formation of protective surface films.[4,10-12] Corrosive attack by high-temperature gases depends strongly on the nature of the films formed by these gases. This relates particularly to the reaction of the base alloy with

components that may diffuse through the films. For example, the protective surface film formed on Fe-Cr-Ni alloys is primarily $Cr_2O_3$.[3,4] In alloys of this type that also contain aluminum, $Al_2O_3$ may form beneath the $Cr_2O_3$ layer[4,8,13-15] with oxygen diffusing through the $Cr_2O_3$ into the base metal and reacting with Al.[4,16,17]

A protective film may fail in service or be degraded by loading stresses, thermally induced stresses, internal growth stresses, abrasion, chemical attack, and changes in the base alloy resulting from diffusion of certain species through the film. For example, $Al_2O_3$ is considered to be generally more resistant than $Cr_2O_3$ to these kinds of attack.[1,8] However, a protective oxide film must depend on in situ reaction to repair itself if ruptured by any means; in this regard, the kinetics of $Cr_2O_3$ reformation are considered superior.[1,8] Healing, as well as the original development of a protective film, will also depend on the environmental species. Where the gas phase is devoid of oxygen sources, or is thermodynamically reducing, the protective oxide films normally associated with specific alloys will not form (or reform) -- and if present, they may decompose. Therefore, protection from gaseous reducing atmospheres by protective films may not be generally expected. The application of artificial surface coatings offers a partial solution to the problem,[18,19] but this may not always be a practical approach.

In this study we evaluated the metallurgical changes caused by exposure of several corrosion-resistant alloys to high-temperature, high-pressure, simple carbonaceous-gas atmospheres. Since these materials normally owe their corrosion resistance to protective oxide films, we examined the influence of prior surface conditions, i.e., as-machined, as-prepolished, and with various preoxidized surfaces. Controlled exposures were conducted in either $CH_4$, CO, or mixtures of the two gases (and their decomposition products) at various temperatures and pressures. Performance was evaluated by examining sample structure and morphology using light microscopy and scanning electron microscopy augumented by some x-ray diffraction and energy-dispersive x-ray analyses. A logical extension of this work would include further analysis and correlation with exposures in more complex environments more closely approximating the actual conditions in in situ coal-gasification processes, for example, gases containing sulfur species or chlorides.

## Experimental

Coupons of eight commercial candidate alloys (Table 1) were exposed to carbonaceous gas mixtures (Table 2)* in a pressure vessel at pressures up to 6.2 MPa and temperatures up to 900°C. The vessel was made of René-41 and had a working cavity 12.8 mm in diameter by 305 mm deep. It was heated by an external, resistance-wound tube furnace. Some 10-12 coupons were exposed during each run by suspending them on a wire (Table 3). Duplicate samples were included to facilitate use of different analytical techniques. The coupons were about 2-3 mm thick by 7.5 mm square, and suspended on a wire through a 0.90-mm-diam hole drilled in the center of the sample face. The samples were separated from each other by 3-mm-thick ceramic-bead insulators (Fig. 1).

The faces of the coupons were polished to a 600-grit lapped finish, while the four sides were exposed in the as-milled surface finish. Selected polished coupons were preoxidized in air at elevated temperatures. Except for the latter heat treatment, all samples were in the as-received, mill-annealed-and-polished condition. Prior to exposure all samples were cleaned with $CCl_4$.

*Differences between the measured and operating gas analyses depend on the chilling effect during gas sample withdrawal. For example, based on thermodynamic calculations, exposure No. 5 should have contained $P_{CO}/P_{CO+CO_2} = 0.31$ as compared to the observed ratio of 0.35. The difference is small.

Table 3. Alloys exposed in the various runs.

| Run No. | Stainless 304 | Stainless 310 | Inconel 601 | Incoloy 800 | Incoloy 811 | Haynes 188 | E-brite 26-1 | Hastelloy X |
|---|---|---|---|---|---|---|---|---|
| 1 | p[a],a[b] | -- | p,a | p,a | p,a | -- | a | -- |
| 2 | a | -- | p,a | p,a | p,a | a | a | -- |
| 3 | a | -- | a | a | a | a | a | -- |
| 4 | a | -- | a | a | a | a | a | -- |
| 5 | a | p,a | a | a | a | a | a | -- |
| 6 | a | p,a | a | a | a | a | a | -- |
| 7 | -- | p,a | a | a | a | a | a | -- |
| 8 | -- | p,a | a | -- | a | a | a | -- |
| 9 | -- | p,a | p,a | -- | a | -- | -- | a |
| 10 | -- | p,a | p,a | -- | -- | -- | -- | -- |

[a]Exposed in some preoxidized form - designated by p.

[b]Exposed in the as-polished form - designated by a.

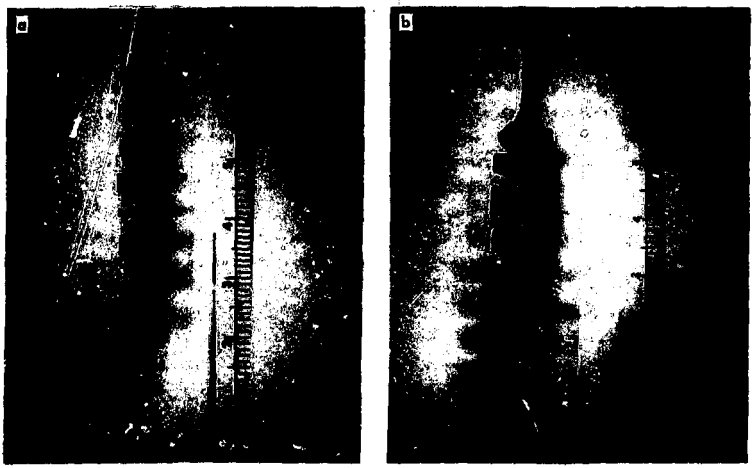


Fig. 1. Suspended arrays of samples, a) before exposure in Run No. 6 b) after exposure in Run No. 5.

Cabonaceous gases of commercial purity were introduced into the pressure vessel at room temperature at relatively low pressures in order to allow for expansion and various decomposition reactions that occur on heating to the exposure temperature. Either pure CO, pure $CH_4$, or a $CO/CH_4$ mixture was charged initially. At the elevated temperatures, these charges decomposed to $CO/CO_2$, $CH_4/C_2$, and $CO/CO_2/CH_4/C_2$ mixtures, respectively. A graphite rod, 12.7-mm in diameter and about 137-mm long, was inserted into the furnace tube to reduce the gas-phase volume and to offset the above decomposition reactions. The resulting gases were, therefore, always equilibrated with respect to carbon (graphite). The vessel typically reached a stable temperature within 2 h, with pressure equilibrated within 3 h.

At the completion of a run (50, 100, or 170 h), a gas sample for composition analysis was withdrawn from the pressure vessel while at the elevated temperature, reducing the pressure by approximately 50%. The furnace was then immediately shut off, cooling to room temperature in about 4 h. Samples were removed taking care not to disturb the surface films.

The exposed samples were evaluated by one or more techniques; these included visual examination, weight-change, x-ray diffraction of the in situ film, scanning electron microscopy, energy dispersive x-ray analysis, and light metallography. Weight-change proved to be an insensitive

measure of corrosion for these exposure conditions, with changes rarely greater than 0.03%; in addition, carbon (soot) deposition on sample surfaces confused the weight measurements. Therefore, the primary measure of corrosion resistance was penetration by corrosion products and changes in the alloy substrate as determined qualitatively by metallographic examination of cross sections. The tops and bottoms of samples tended to collect differing amounts of loose soot because of the sample-handling arrangement. Thorough comparison of morphology and metallography of top and bottom sample faces assured that the tops and bottoms were equivalent; loose soot did not appear to affect corrosion behavior.

## Results and Discussion

The macroscopic appearance of the exposed coupons varied from light-colored tarnishes to black-soot deposits. Not all of the exposed samples were examined metallographically, but the 310 stainless steel (310 SS) and Inconel 601 coupons were examined in great detail. No general correlation was found between the microscopic and external macroscopic appearances.

### CARBON-MONOXIDE/METHANE EXPOSURES — LIGHT MICROSCOPY

Metallographic examination of cross sections of samples exposed to CO or CO/$CH_4$ (initial) gas mixtures generally revealed the development of three diffusion-corrosion zones: (1) a structureless, grey-etching, usually continuous surface layer, (2) a light-etching sublayer usually consisting of small equiaxed light-etching grains about 1-3 grains thick and at times peppered with precipitates, and (3) below this a region of general precipitation and/or grain boundary precipitation in the base metal. At times the grain boundary precipitation extended to the surface layer, and solute depletion was also apparent in the sublayer.

No attempt was made to identify the constituents (oxides or carbides) present. On the basis of the Boudouard reaction ($2CO \rightarrow C + CO_2$) which reached equilibrium as evidenced by soot deposition, NiO could not have formed at the surface, and if present there originally (due to preoxidation), it should have decomposed.

Oxides of irons are probably stable under the conditions used; e.g., calculations using the free energy data for the Boudouerd reaction shows that for run No. 10 (CO addition at 700°C, 6.2 MPa) the equilibrated $CO/CO_2$ ratio is 0.11 which falls within the region where $Fe_3O_4$ is the stable phase. If the temperature were increased to 900°C, FeO would be the more stable phase; if it were increased to 1000°C, the $CO/CO_2$ ratio becomes 0.720 and no oxide of iron should form.

With respect to chromium, $Cr_2O_3$ should readily form in all of the exposures containing CO. The formation of a carbide, possibly $Cr_{23}C_6$, should also occur. The $CO/CO_2$ ratios obtained are reducing towards

the carbide but oxidizing relative to the oxide, i.e., both species may coexist. Finally, $Al_2O_3$ will always form. Carbides of Ni and Al will not be stable and should not form, also $Fe_3C$ should not form from the gas phase under the conditions used. Therefore we assume that, in general, the surface oxides are predominantly $Cr_2O_3$ with some $Al_2O_3$ together with various oxides of iron.

Precipitates at the grain boundaries and within the grains are probably predominantly carbides. Some internal oxidation, especially for the preoxidized samples, would also be expected. As will be shown, the light-etching granular sublayer could be ascribed to either oxides or carbides depending on the exposure conditions.

The general features described in the above may be seen in Fig. 2, which contains

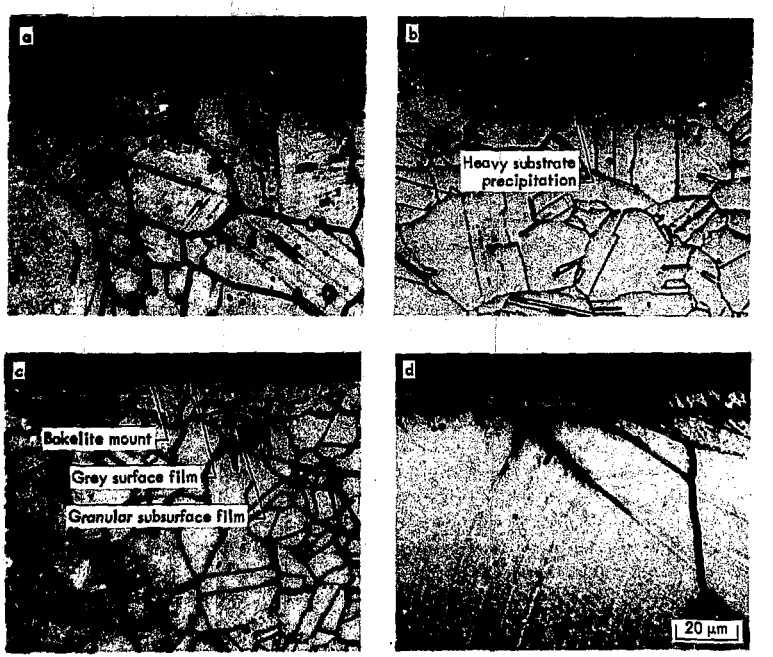


Fig. 2. Microstructures illustrating typical surface attack. All samples exposed in Run No. 8, a) Haynes 188, b) Incoloy 811, c) 310 SS, d) Inconel 601.

cross sections* of several alloys showing corrosion attack of as-polished, nonpreoxidized coupons exposed to Run No. 8 (50 CO/50 $CH_4$ charge at 700°C, 5.5 MPa). We could not observe any systematic trends with respect to temperature or pressure or to the addition of $CH_4$ to CO. We noted, however, that the sides (milled finish) invariably suffered deeper penetration by the corrosion products than did the polished surfaces.

Figure 3 contains micrographs of 310 SS samples: (a) as preoxidized 100 h at 700°C;† (b) preoxidized plus exposure to Run No. 10 (CO charge at 700°C, 6.2 MPa); and (c) Run No. 10 only. The top edge of each view corresponds to the polished surface while the right-hand side corresponds to the as-machined milled surface. Although the preoxidation treatment appeared to accentuate the penetration at the milled surfaces, the amount of internal precipitation below the polished surface was decreased by this treatment (compare views 3b and 3c). We noted that preoxidation at a lower temperature of 500°C had no significant affect on corrosion attack. An intermediate preoxidation temperature (700°C) usually improved the resistance to corrosion at polished surfaces, and high preoxidation temperatures ($\geq$ 1000°C) were always detrimental.

Differences due to the preoxidation treatments observed on the polished surfaces of 310 SS may be seen more clearly in Fig. 4 which contains photomicrographs

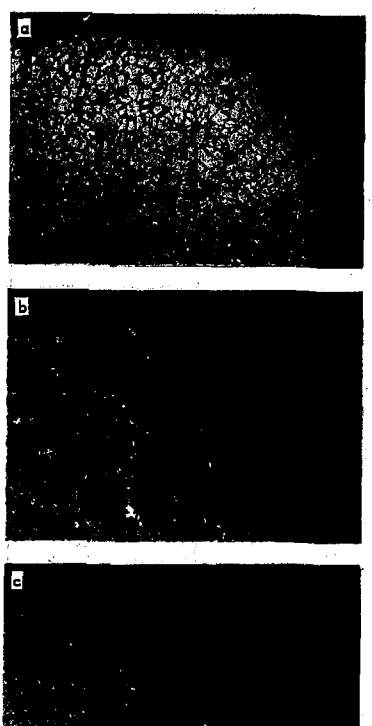


Fig. 3. Photomicrographs of 310 SS exposed to various combinations of environments, a) 100 h at 700°C in air, b) 100 h at 700°C in air followed by Run No. 10, c) Run No. 10 alone. Top of each view is original polished surface, right side is original machined surface.

*Unless otherwise indicated, all cross sections show the effect of exposure of the as-polished surface.

†Preoxidation was accomplished by heating in air.

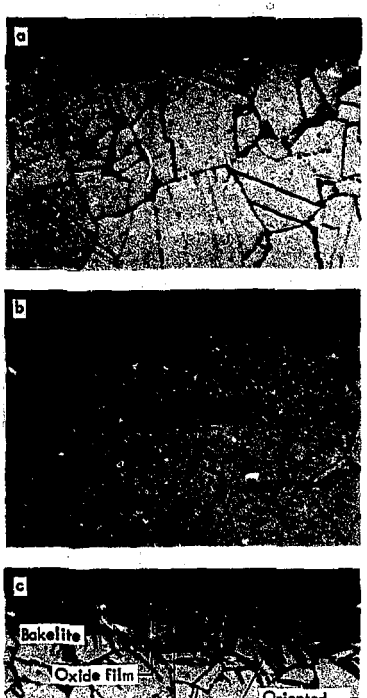


Fig. 4. Photomicrographs showing differences obtained in 310 SS samples as a result of preoxidation, a) as preoxidized 100 h at 700°C in air, b) preoxidized plus exposure to Run No. 10, c) not preoxidized, exposed only to Run No. 10, all a higher magnification than Fig. 3.

of the samples shown in Fig. 3 but at a higher magnification. The granular sublayer appears thickest for the combined preoxidized and carbonaceous exposure and finest for the carbonaceous exposure alone. This would suggest that this sublayer probably contains some oxide. In the absence of the preoxidation treatment, carbide precipitates formed which are arranged in crystallographically oriented arrays penetrating some 20 µm below the surface (view 4c). This was also seen in the preoxidized sample but to a much lesser extent and with less penetration. Such differences between preoxidized and non-preoxidized samples can be ascribed to the oxides acting as diffusion barriers between the carbon supplied by the gas phase and the matrix alloy elements (especially Cr).

The effect of an excessive preoxidation temperature is seen in Fig. 5 for 310 SS exposed 1 h in air at 1121°C and water quenched. A segmented, relatively thick, irregular surface film is obtained. No granular oxide sublayer developed although grain boundary and internal oxidation had occurred (the water quench should have prevented carbide precipitation on cooling from 1121°C), as may be seen in the as-polished (5a) and lightly etched (5b) views. Etching sufficient to bring out the austenitic alloy structure (view 5c) results in a severly overetched zone below the surface film suggesting extensive Cr depletion in that zone.

The effect of an excessive preoxidation temperature for inconel 601 is shown at two magnifications (200 and 750X) in Fig. 6. The preoxidation treatment was 3 h at 1000°C in air; the carbonaceous exposure was in Run No. 10 (CO charge,

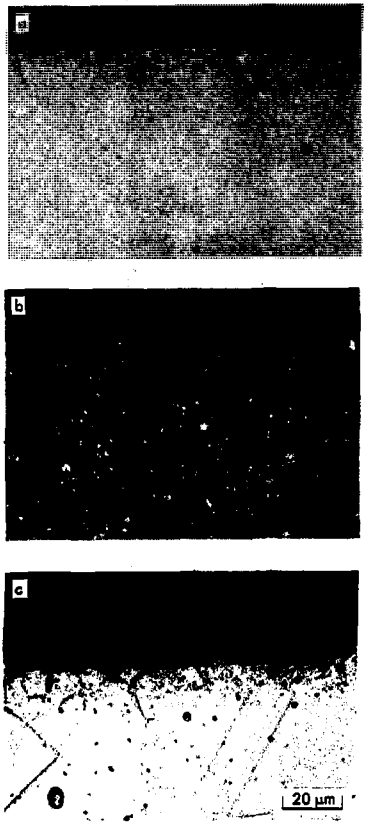


Fig. 5. Photomicrographs showing the formation of a discontinuous oxide film and substrate precipitation in 310 SS exposed for 1 h at 1121°C in air, *a)* as-polished, b) light etch, c) heavy etch of exposed samples.

700°C, 6.2 MPa). Two of the structures, (a) preoxidized and (b) preoxidized and carbonaceous exposure, appear very similar with respect to the formation of a surface film and internal oxidation and/or carbide precipitation. Both samples also contain a thin sublayer of very fine grains, about one grain thick, just below the surface film. Evidence of a solute-depleted zone, about 27 μm thick, can be seen in both samples, but of the two this appears to be most evident in the preoxidized and carbonaceous-exposed sample. The sample exposed only to the carbonaceous atmosphere (view 6c) showed considerably less penetration of the corrosion products than did either of the other two, particularly with reference to thickness of surface film, depth of solute depletion, and extent of precipitation or internal oxidation. In comparing the three samples in Fig. 6, it appears that the main differences arise as a result of the test temperatures, i.e., the 1000°C preoxidation versus the 700°C carbonaceous exposure, the former causing much deeper penetration of the corrosion products including solute depletion. The surface film of the preoxidized sample may have played a role in limiting the growth of the granular sublayer since it is thickest for the carbonaceous exposure only.

We next examined whether preoxidation of Inconel 601 at the same temperature as that used in the subsequent carbonaceous exposure would minimize the carbonaceous atmosphere attack. Figure 7 shows views of three samples of Inconel 601 exposed to three different 700°C treatments: (a) 100 h in air, (b) run No. 10 (100 h in CO charge at 700°C, 6.2 MPa), and (c) 100 h in air followed by run No. 10.

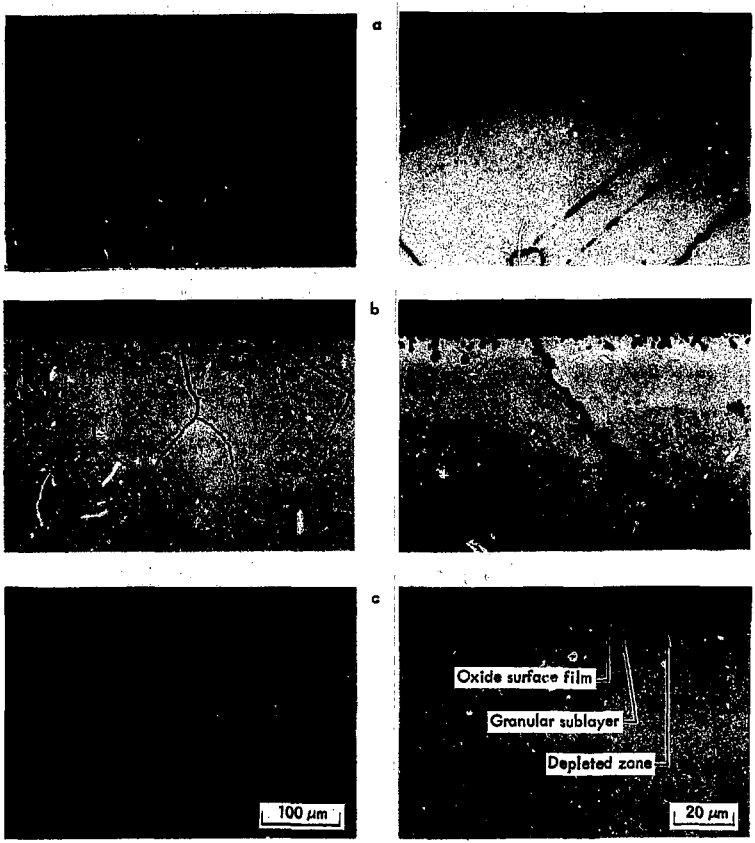


Fig. 6. Photomicrographs of Inconel 601 samples exposed to various conditions, a) 3 h in air at 1000°C, b) 3 h in air at 1000°C followed by exposure in Run No. 10, c) exposed in Run No. 10 only.

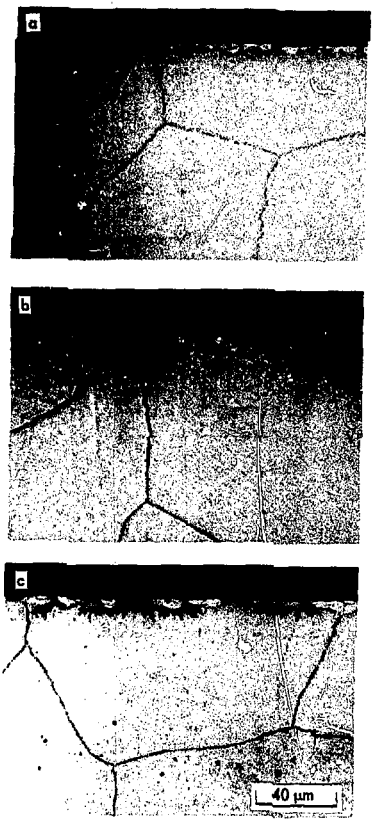


Fig. 7. Photomicrographs of Inconel 601 samples exposed to three different 700°C treatments, a) 100 h in air at 700°C, b) Run No. 10 only, c) 100 h in air at 700°C followed by exposure in Run No. 10.

Very little difference is seen in the microstructures between the preoxidized and carbonaceous exposures (views 7a, b). The two successive exposures (view 7c) resulted in additional penetration by corrosion products especially with respect to the degree of precipitation. Thus, in contrast to the beneficial effects obtained with the 700°C preoxidation treatment for 310 SS, no visual evidence of improvement appeared for Inconel 601.

METHANE EXPOSURES -- LIGHT MICROSCOPY

Figure 8 shows the microstructures of Inconel 601 samples that were obtained following exposure to (a) Run No. 1 ($CH_4$ charge at 600°C, 4.8 MPa), (b) No. 6 ($CH_4$ charge at 700°C, 41 MPa) and (c) No. 2 ($CH_4$ charge at 800°C, 4.8 MPa). These samples were not preoxidized. As with those samples exposed to CO and CO/$CH_4$ charges, three main corrosion zones were observed in the microstructure: (a) a grey-etching structureless surface film, (b) a light-etching granualr sublayer, and (c) precipitation penetrating into the substrate. The degree of penetration or thickness of each of these zones increases with an increase in temperature. This is especially so with respect to (carbide) precipitation.

The effects of a preoxidation treatment are further illustrated in Fig. 9. Exposure for 24 h at 1000°C in air resulted in the formation of a thick, irregular, grey film (view 9a) which was partially reduced and/or fragmented on subsequent exposure to the $CH_4/H_2$ gas mixture of run No. 1 (view 9b). In comparing the two samples, several interesting features may be seen. In both samples, intrusions from

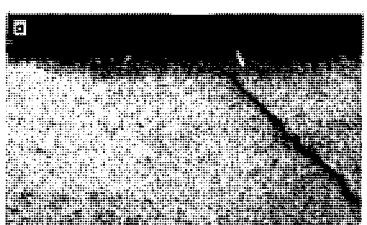


Fig. 8. Photomicrographs of Inconel 601 samples exposed to $CH_4/H_2$ gas mixtures, a) Run No. 1, 600°C, 170 h, 4.8 MPa, b) Run No. 6, 700°C, 100 h, 4.8 MPa, c) Run No. 2, 800°C, 100 h, 4.1 MPa. Samples were not preoxidized.


Fig. 9. Photomicrographs of Inconel 601 samples, a) as preoxidized at 1000°C in air for 24 h, b) preoxidized at 1000°C in air for 24 h and exposed to Run No. 1.

the grey oxide film into the substrate were noted, especially at the austenite grain boundaries. In comparing views (9a) and (9b), these intrusions obviously occurred during the preoxidation treatment. The austenite grain boundaries could not readily be detected in the preoxidized sample for a depth of about 30 µm below

the surface. Evidently, the carbides delineating these grain boundaries had been eliminated by the oxidation process, either by being directly oxidized or through the reaction of oxygen with Cr yielding a Cr-depleted zone and resulting in the $Cr_xC_y$ going into solution. However, the intrusion of the oxide at the top of view 9a reasonably corresponds to the extension of a grain boundary from what would appear to be a triple point of the austenite grain boundaries. Upon subsequent exposure to the carbonaceous atmosphere of Run No. 1 ($CH_4$ charge, 600°C, 4.8 MPa), the enrichment of carbon and the arrival of Cr, either from the interior of the sample or by the reduction of $Cr_2O_3$, again result in $Cr_xC_y$ grain boundary precipitation with the complete delineation of the austenite grain boundaries. In comparing Fig. 9 with Fig. 8a (both samples were exposed to Run No. 1), it is observed that the preoxidation treatment has resulted in more extensive sublayer growth (light-etching granular structure). Evidence of sublayer activity is seen in the preoxidized sample of Fig. 9a. Thus, one may conclude that prior Cr-depletion (i.e., $Cr_2O_3$ formation) permitted more rapid attack on subsequent exposure to the $CH_4/H_2$ atmosphere.

## SCANNING ELECTRON MICROSCOPE EXAMINATION OF SURFACES

Selected sample surfaces were examined by Scanning Electron Microscopy (SEM) to determine through recognizable morphology, the type of outer-layer compounds and to reveal surface features such as film continuity, cracks, soot, and the distribution of various phases.

As noted earlier, varying the preoxidation temperature may produce significant differences in the initial film and in its performance in carbonaceous gases. For example 310 SS, when preoxidized at 700°C, develops a macroscopically coherent film (Fig. 10a) including an outer layer consisting of numerous microscopic NiO {111}-faced hillock crystals. However, pretreatment at 1000°C leads to scale cracking and spalling (upon cooling) with subsequent exposure of the base metal (Fig. 10b). The visual appearance of the 1000°C-exposed 310 SS samples also reflected this fine-scale cracking; the 1000°C-oxidized surface had a dull gray "pocked" or "sand-blasted" appearance while the 700°C oxide film was smooth and coherent. A further undesirable manifestation of the 1000°C preoxidation exposure of 310 SS was a tendency to promote significantly more surface carbon (soot) deposition than that resulting from preoxidation at lower temperatures. This behavior may be related to increased NiO external scale formation at 1000°C, which on subsequent decomposition on exposure to reducing conditions would give rise to a high surface concentration of nickel as a catalytic cracking agent for the carbonaceous gases. Such enhanced methane decomposition may have a significant effect on the efficiency of gas production for a coal gasification process. Thus, in addition to corrosion protection, the specific nature and distribution of film compounds should also be considered.

Spalling of initially coherent surface films was also observed in many cases after carbonaceous gas exposure. Evidence of spalling is shown in Fig. 11 for a sample of 310 SS preoxidized in air 3 h at 500°C

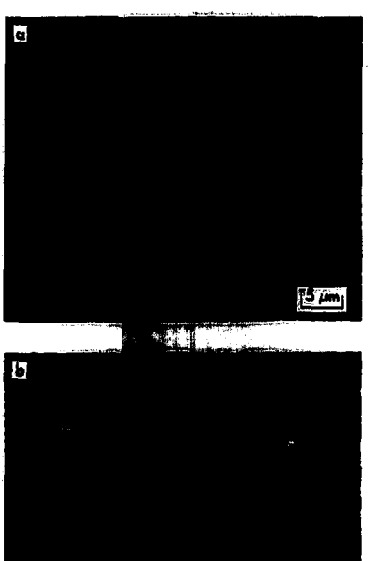


Fig. 10. Surface topography of 310 SS samples following exposure in air (preoxidation), a) 100 h at 700°C, b) 3 h at 1000°C.

and then exposed to Run No. 6 ($CH_4$ charge, 700°C, 4.8 MPa). The origin of the macroscopically "pebbled" external scale structure in view 11a can be deduced from higher magnification SEM examination of the scale underside (view 11b) obtained from a piece of spalled scale mounted to expose the scale/base metal interface. The array of holes in the scale (a higher magnification view of one hole is shown in view 11c) corresponds to the points where the scale adhered to the base metal, with the nonadherent scale "ballooning" or "tenting" between these fixed points. The missing patches of scale can be observed on the exposed base metal surface of the sample (view 11d). These adherent patches were obviously too small to prevent general macroscopic flaking of the scale. This spalling may result from the development of growth stresses in the surface film at high temperature or from differential thermal contraction on cooling from the exposure temperature. In either case, 310 SS is unlikely to maintain a natural protective film under these conditions. Additional examination at high magnification of the samples shown in Fig. 11 indicates that the originally coherent preoxidation film (such as in view a) has become microscopically porous from reduction of the original film compounds. These observations indicate that carbonaceous gases may have a devasting effect on the performance of contemporary alloys at normally servicable temperatures. Furthermore, the conditions to which materials have been subjected in these preliminary exposures are comparatively mild compared with many actual service environments (such as in coal conversion processes) where gas flow, stress, abrasion, and other environmental agents are added factors.

Other alloys have similar film reactions with carbonaceous gases. Figure 12 demonstrates the effect of carbonaceous gas exposure on preoxidized Inconel 601. The individual particles of the preoxidized surface oxide seen in view 12a appear in view 12b to be eroded by the exposure to Run No. 9 (50CO/50$CH_4$ charge, 700°C, 6.2

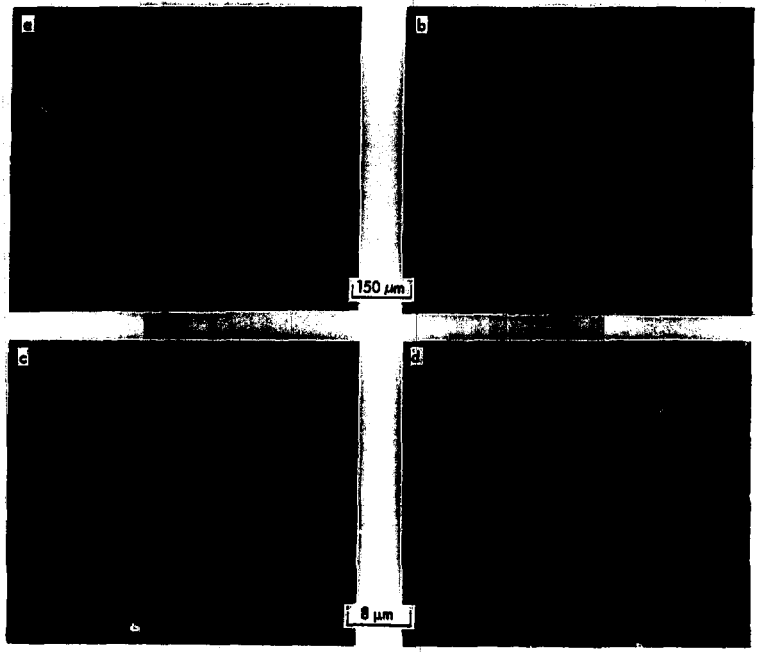


Fig. 11. Surface and undersurface topography of films from a sample of 310 SS, first preoxidized by heating for 3 h at 500°C in air and then exposed to Run No. 6, a) partially spalled film surface, b) underside of piece of spalled scale, c) view of one hole seen in b), d) patch of film corresponding to hole of view c) retained on metal surface.

MPa). Under these conditions one of the initial scale oxides has been apparently selectively reduced and, therefore, removed from the film. The absence of the familiar triangular-faced NiO hillocks suggests that the external NiO phase was reduced as in the case of 310 SS. This is consistent with the relative thermodynamic stabilities of various oxides.

The white globular areas in view 12b probably are $Al_2O_3$. In Inconel 601, $Al_2O_3$ is formed in greater proportion at grain

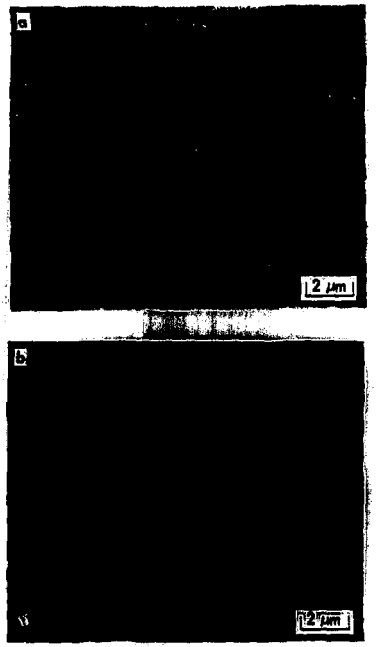


Fig. 12. Surface topography of two Inconel samples showing attack of a preoxidized surface, a) as preoxidized 3 h at 1000°C in air, b) subsequently exposed to Run No. 9.

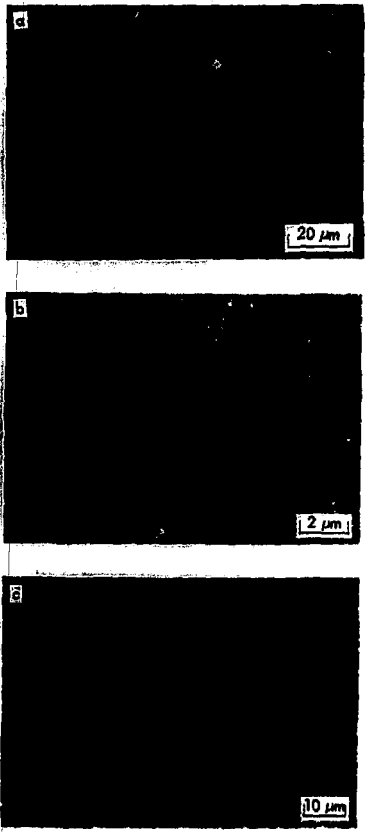


Fig. 13. Views illustrating relation of film characteristics to substrate grain boundaries for Inconel 601 preoxidized by heating for 3 h at 1000°C in air followed by exposure in: a) and b) Run No. 9, c) Run No. 2.

boundaries as seen in Fig. 13, views a and b. Therefore, while $Al_2O_3$ may form a useful surface film in terms of resistance to reduction by carbonaceous gas atmospheres, the alloy composition of Inconel 601 (1.35 wt% Al) contains insufficient Al for a complete layer of $Al_2O_3$. Similarly, Incoloy 800 (0.5 wt% Al)

and Incoloy 811 (1.75 wt% Al) probably would not retain or form compact $Al_2O_3$ films in carbon-rich atmospheres.

Nonuniform film formation resulting from underlying microstructural features is demonstrated in Fig. 13, view c. The "bare patch" evident near the grain boundary obviously corresponds to an underlying MC-type carbide particle. Energy dispersive x-ray analysis (EDA) of films on the normal internal grains ($\gamma$ and $\gamma'$) and on the "bare patch" (MC carbide) showed that the film over $\gamma$ and $\gamma'$ is richer in Ti and poorer in Al than is the film covering the MC carbide.

Figure 14 illustrates the relative surface deterioration suffered by nonpreoxidized samples in Inconel 601 (a), Incoloy 811 (b), 310 SS (c) and (d) exposed in Run No. 8 (50 CO/50 $CH_4$, 700°C, 5.5 MPa). The former two Ni-rich alloys seem to be somewhat less prone to deterioration in the

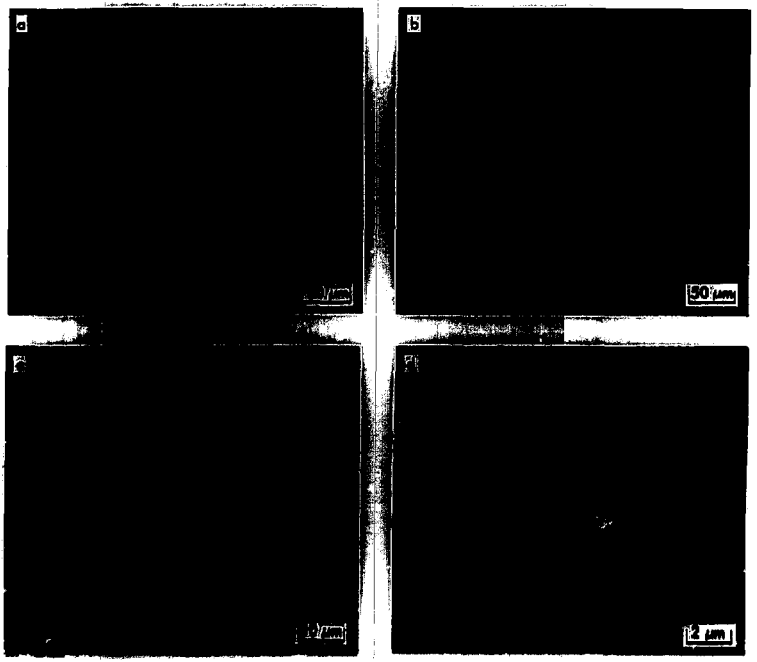


Fig. 14. Relative surface deterioration of unpreoxidized samples, a) Inconel 601, b) Incoloy 811, c) 310 SS, d) 310 SS enlarged. All exposed to Run No. 8.

carbonaceous atmosphere than the 310 SS. The 310 SS at low magnification (c) shows an eroded-like surface which at higher magnification (d) indicates an apparent conversion to filamentary carbides. The "debris" on the surface in views 14a and 14b is deposited soot. Note that the exposure conditions for these samples correspond closely to those associated with the deterioration phenomena known as "metal dusting" which proceeds apparently by a conjoint oxidation-reduction reaction.[20-27] In this case, the gas analysis ($CO/CO_2/CH_4/H_2$, 15.2/21.6/52.5/10.6) supports the possibility of such a mechanism.

The superior performance of Inconel 601 and Incoloy 811 in these environments may be realted to the presence of the more stable $Al_2O_3$ phase in the film, as discussed earlier. In this regard, Incoloy 811 might be expected to be more satisfactory than Inconel 601 because of the higher Al content (1.75 wt% vs. 1.35 wt%) although in both alloys the Al content is inadequate. However, metallographic examinations indicate somewhat more nonuniform films for Incoloy 811, indicating that these low Al contents in the compositions alone are not the determining factor, and that the relative rates of diffusion and reaction and the distribution of various phases are particularly important.

The possibility of using a less expensive material such as low-carbon steel in high temperature carbonaceous atmospheres was dramatically shown to be inappropriate. In one case a sample of a plain low-carbon steel, exposed to Run No. 4 (CO charge 600°C, 4.5 MPa for 170 h, exhibited a remarkable transformation to a very carbon-rich friable material, which is a manifestation of advanced graphitization. This behavior was observed only in the $CO/CO_2$-containing atmospheres. In the $CH_4/H_2$ mixture the surfaces were "reduction-etched," producing a flake-like scale (see Fig. 15). Thus the rate of destruction of the unalloyed steels in carbonaceous atmospheres is greatly dependent on the atmospheric composition and such destruction may be catastrophic.

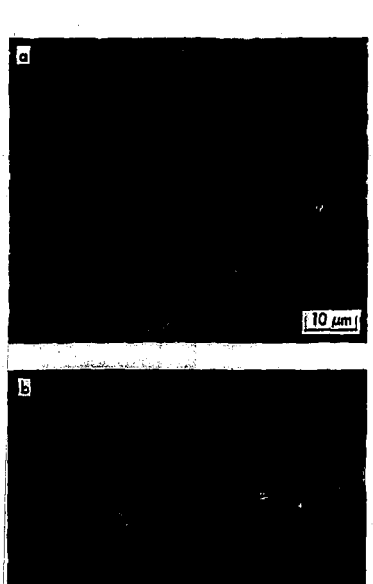


Fig. 15. Flake-like topography resulting from exposure of a SAE 1018 steel in Run No. 3 ($CH_4$ charge), two different magnifications.

## Some Concluding Comments

The original purpose of this study was to become familiar with the types of film formation and corrosive attack that might be encountered when particular alloys are exposed to carbonaceous environments; this goal was accomplished. Further, some ranking of these materials was anticipated. The limited scope of the investigation to date did not provide sufficient information to adequately do this, although the observations indicate that Al may be an important and necessary alloying constituent for resisting attack under reducing conditions.

Most importantly, surface films and subsurface precipitates need to be identified by x-ray and electron diffraction. Chemical analysis as a function of substrate depth would have to be obtained to determine the extent of solute depletion. One must decide what is more significant in degrading the material: solute depletion, precipitation, grain boundary attack, or general metal loss. To adequately answer these questions, in addition to more extensive surface and substrate analyses, one must also resort to mechanical testing.

From a practical point of view, the reaction of these materials to actual burning-coal and gas-product environments may be quite different than the behavior observed in this study. This was dramatically demonstrated for a low-carbon steel, which showed catastrophic attack in the $CO/CO_2$ atmosphere in contrast to the much slower attack obtained in the $CH_4/H_2$ atmosphere, both relatively mild compared to the anticipated coal gasification environments. A variety of morphologies, both in the cross sections and in the topographic views were obtained for the high-temperature alloys. These were affected by the preoxidation, the carbonaceous exposure environment, and the alloy composition. Although we hesitate to rate these materials on the basis of our limited observations, nevertheless, this study should provide some background for future work involving materials screening, materials mechanical properties evaluation, and basic corrosion studies.

## Acknowledgments

The authors wish to thank E. O. Snell and S. A. McInturff for their metallographic support.

# References


1. G. E. Wasilewski and R. A. Rapp, "High Temperature Oxidation," in The Superalloys C. T. Sims and W. C. Hagel Eds. (Wiley, N.Y., 1972) pp. 287-315.
2. D. L. Douglass, "Fundamentals of the Reactions Between Metals and their Environment at High Temperatures," in Materials 1971 (SAMPE, 1971) p. 1.
3. I. G. Wright, "Oxidation of Iron-, Nickel-, and Cobalt-Base Alloys," Metals and Ceramics Information Center, Battelle Columbus Laboratories, Rept. 72-07 (1972).
4. G. C. Wood, Oxidation Metals 2, 11 (1970).
5. R. C. Logani and W. W. Smeltzer, Can. Metalworking 10, 149 (1971).
6. G. C. Wood, "The Structures of Thick Scales on Alloys," in Proc. Seminar Oxidation Metals Alloys, Metals Park, Ohio, 1971 (ASM, 1971) pp. 201-234.
7. F. C. Schora, Jr., "Materials and Corrosion Considerations in the IGT Hygass Process," in Proc. Workshop on Materials Problems and Research Opportunities in Coal Gasification, Ohio State University, (NSF, 1974) pp. 163-188.
8. R. A. Rapp, "High-Temperature Gaseous Corrosion of Metals in Mixed Environments" ibid. pp. 313-334.
9. A. M. Hall, Mater. Design Eng. 80, 16 (1974).
10. P. Hamock, "What is the Role of Stress in Oxidation," in High Temperature Corrosion of Aerospace Alloys, J. Stringer, R. Jaffee, and T. F. Kearns, Eds., AGARD Conf. Proc. 120 (1973) p. 117.
11. C. S. Giggins, B. H. Kear, F. S. Pettit, and J. K. Tien, Met. Trans. 5, 1685 (1974).
12. D. L. Douglass, "Exfoliation and the Mechanical Behavior of Scales," University of California at Los Angeles, Rept. UCLA-ENG-7105 (1971).
13. W. C. Hagel, Corrosion 21, 316 (1965).
14. F. S. Pettit, "On the Effects of Oxide Dispersions and Rare Earth Type Elements in the Oxidation of Cr and Al-containing Alloys," in High Temperature Corrosion of Aeropsace Alloys, J. Stringer, R. I. Jaffee, and T. F. Kearns, Eds., AGARD Conf. Proc. 120 (1973) p. 156.
15. A. Davin and D. Coutsouradis, "What are the Effects of Alloying Elements Singly or in Combination in Hot Corrosion," ibid. p. 222.
16. F. H. Scott, G. C. Wood, and M. G. Hobby, Oxidation Metals 3, 103 (1971).
17. F. H. Scott and G. C. Wood, Corrosion Sci. 11, 799 (1971).
18. S. J. Grisaffe, "Coatings and Protection," in The Superalloys, C. T. Sims and W. C. Hagel, Eds. (Wiley, N. Y. 1972) pp. 341-370.
19. M. A. Gedwill and S. J. Grisaffe, Metals Eng. Quart. 12 (2), 55 (1972).
20. R. F. Hochman, "Oil-Ash Corrosion of Alloy Steels at High Temperatures," in Proc. Intern. Congr. Metallic Corrosion, 4th (NACE, 1972) p. 258.

21. R. F. Hockman, Catastrophic Deterioration of Metals in Carbonaceous Environments (NACE, September 1973).
22. P. A. LeFrancois and W. B. Hoyt, Corrosion 19, 360 (1963).
23. N. Birks, Brit. Corrosion J. 3, 56 (1968).
24. W. B. Jepson, J. E. Antill, and J. B. Warburton, Brit. Corrosion J. 1, 15 (1965).
25. J. E. Antill and J. B. Warburton, Corrosion Sci. 7, 645 (1967).
26. H. C. Cowen and C. Tyzack, Brit. Corrosion J. 3, 220 (1968).
27. I. A. Menzies and W. J. Tomlinson, Brit. Corrosion J. 2, 235 (1967).

RBC/gw